# Surface Plasmon Resonance Multisensing

**ARTICLE** *in* ANALYTICAL CHEMISTRY · JANUARY 1998

Impact Factor: 5.64 · DOI: 10.1021/ac970929a



**4 AUTHORS**, INCLUDING:

Charles E. H. Berger
Netherlands Forensic Institute
**32** PUBLICATIONS **503** CITATIONS
SEE PROFILE

Tom a Beumer
ELITech Group
**13** PUBLICATIONS **330** CITATIONS
SEE PROFILE

Jan Greve
University of Twente
**304** PUBLICATIONS **8,823** CITATIONS
SEE PROFILE

*Anal. Chem.* **1998,** *70,* 703−706

# Surface Plasmon Resonance Multisensing

Charles E. H. Berger,[†,‡] Tom A. M. Beumer,[§] Rob P. H. Kooyman,[*,†] and Jan Greve[†]

*Department of Applied Physics, MESA Institute, Bio-interface Group, University of Twente, P.O. Box 217, 7500 AE Enschede, The Netherlands, and Organon Teknika BV/AKZONOBEL, P.O. Box 84, 5280 AB Boxtel, The Netherlands*

**We have demonstrated the feasibility of surface plasmon resonance (SPR) multisensing by monitoring four separate immunoreactions simultaneously in real time using a multichannel SPR instrument. A plasmon carrying gold layer, onto which a four-channel flow cell was pressed, was imaged at a fixed angle of incidence. First, the four-channels were coated with antibodies and then the flow cell was turned by 90° such that the flow channels overlapped the areas coated in the first step. In that geometry, antigens were applied to the different antibodies on the surface. Thus, all antibody−antigen combinations can be measured in a two-dimensional array of sensor surfaces in real time. Our results do correlate with expected immunologic specificity. The emphasis will be on presenting this method to obtain data on immunosystems and not as much on the assessment of biological activity.**

In recent years, progress has been made in the field of optical evanescent field immunosensors. With these sensors, biomolecular interactions within the evanescent field volume are detected via a change in the refractive index or layer thickness at the sensor surface. Thus, labeling of biomaterials is not required. The shift in the condition for the excitation of surface plasmons has often been used as a sensing principle.[1−3] Different detection principles have been used to detect this resonant excitation.

Angular scans using a rotation table offer the possibility of using Fresnel theory to obtain the layer parameters from a fit of the reflected intensity as a function of the angle of incidence over a large range of angles. A single scan, however, usually takes several minutes and thus even slow changes cannot be monitored in real time.[4,5] Angular scans can be sped up by using a scanning mirror.[6]

Another method is to measure the reflectance curve by using a convergent light beam covering a suitable range of incidence angles reflected at the prism base and imaged onto a photodiode array. The resonance angle can then be determined from the position of the reflectance minimum on the detector array (using a fitting algorithm).[7]

A third possibility is to use the wavelength dependence of surface plasmon resonance (SPR). The angle of incidence is kept fixed and a broad-band light source is used. Only one wavelength will couple to the SP, and a spectral analysis of the reflected light will show an absorption dip at this wavelength.[8,9] Using an acousto-optic tunable filter (AOTF), the differential reflectivity as a function of the wavelength has been measured.[10]

Probably, the most straightforward method is to keep the incident angle fixed at a value for which the reflectance is halfway down its minimum and to monitor changes in reflectance.[1,3,11] The latter method was chosen for the multichannel SPR sensing experiments described in this paper.

There are a number of reasons why multichannel immunosensing is desirable: (i) simultaneous measurements save time; (ii) leading a solution past a number of sensor surfaces is preferred when only a low sample volume is available; (iii) multianalyte mixtures can be measured and pattern recognition becomes feasible; (iv) reference and duplicate measurements can easily be included; (v) sensor areas are identical for all measurements which reduces variations.

Because SPs have a short propagation length[12] (for gold and in the visible part of the spectrum typically in the micrometer range), they are particularly well suited for imaging a two-dimensional array of small sensing areas with surface dimensions exceeding the propagation length. All sensing areas can be present at the same sensor surface, and the imaging system allows simultaneous and independent measurements to be made on different locations of the sensor surface. The fact that the sensor surfaces can be visually observed in real time (and thus problems such as passing air bubbles can be detected) is a practical advantage of this method. By recording the images on video tape,

* Corresponding author: (tel) -31-53-4893157; (fax) -31-53-4891105; (e-mail) r.p.h.kooyman@tn.utwente.nl.

† University of Twente.

‡ Current address: Department of Chemical Engineering & Materials Science, University of California, Davis, Davis, CA 95616-5294; (tel) (530) 752-6452; (fax) (530) 752-1031; (e-mail) ceberger@ucdavis.edu.

§ Organon Tecknika BV/AKZONOBEL.

(1) Daniels, P. B.; Deacon, J. K.; Eddowes, M. J.; Pedley, D. G. *Sens. Actuators* **1988**, *15*, 11−18.

(2) Flanagan, M. T.; Pantell, R. H. *Electron. Lett.* **1984**, *20*, 968−970.

(3) Liedberg, B.; Nylander, C.; Lundström, I. *Sens. Actuators* **1983**, *4*, 299−304.

(4) Brink, G.; Sigl, H.; Sackmann, E. *Sens. Actuators, B* **1995**, *24−25*, 756−761.

(5) Pollard, J. D.; Sambles J. R. *Opt. Commun.* **1987**, *64*, 529−533.

(6) Lenferink, A. T. M.; Kooyman, R. P. H.; Greve, J. *Sens. Actuators, B* **1991**, *3*, 261−265.

(7) Ivarsson, B.; Jönsson, U.; Karlsson, R.; Liedberg, B.; Renck, B.; Roos, H.; Sjödin, H.; Stenberg, E.; Ståhlberg, R.; Urbaniczky, C.; Lundström, I. *Proceedings of the 3rd International Meeting on Chemical Sensors*; Cleveland, Sept 24−26, 1990; pp 157−160.

(8) Katerkamp, A.; Bolsmann, P.; Niggemann, M.; Pellmann, M.; Cammann, K. *Mikrochim. Acta* **1995**, *119*, 63−72.

(9) Zhang, L.-M.; Uttamchandani, D. *Electron. Lett.* **1988**, *24*, 1469−1470.

(10) Jory, M. J.; Bradberry, G. W.; Cann, P. S.; Sambles, J. R. *Meas. Sci. Technol.* **1995**, *6*, 1193−1200.

(11) Jordan, C. E.; Corn, R. M. *Anal. Chem.* **1997**, *69*, 1449−1456.

(12) Berger, C. E. H.; Kooyman, R. P. H.; Greve, J. *Rev. Sci. Instrum.* **1994**, *65*, 2829−2836.

S0003-2700(97)00929-3 CCC: $15.00 
Published on Web 01/21/1998

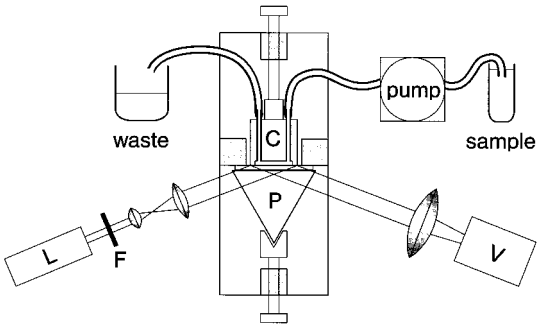


Figure 1. Schematic representation of the setup used for the multichannel measurements: L, HeNe laser; F, gray filter; P, prism; C, multichannel flow cell; V, video camera.

the exact size and position of the sensor surfaces can also be selected after the measurements. Other advantages are the inherent optical sensitivity of surface plasmons and the instrumentational simplicity. Finally, because small sensor surfaces can be defined, relatively few molecules are needed to obtain a certain surface density.

## EXPERIMENTAL SECTION

The experimental setup is shown in Figure 1. The sample delivery system consisted of a four-channel flow cell and four-channel peristaltic pump. The flow rate used was 4.9 mL/h. Layers of 2-nm Ti followed by 47.8-nm Au were evaporated onto a glass slide, which was brought in contact with a prism (BK7 glass; $n = 1.515$), using a suitable index matching oil. A light beam from a 2 mW HeNe laser ($\lambda = 632.8$ nm) was expanded to a 2-cm diameter and attenuated by a factor of 300. The angle of incidence was chosen slightly to the left of the minimum in the SPR reflectance curve; therefore the increase in reflectance will be approximately linear with the increase in layer thickness (see Figure 2). Assuming that the refractive indices of the used antibodies and antigens are similar, the measured reflectance is proportional to the mass bound to the surface. After internal reflection in the prism, the light was imaged by a large-diameter lens ($f = 90$ mm) on a CCD video camera with a linear response (VCM 3250; Philips). Therefore, the beam's intensity profile and the possible presence of air bubbles could be checked at all times. As the reflectance signal is proportional to the incident intensity, it is important to have a flat profile. Images were recorded on videotape for later analysis. A video digitizer (VisionPlus AT OFG; Imaging Technology, Inc., Woburn, MA) was used to calculate the average intensity of the defined sensor areas in the image as a function of time when the tape was played back. All chemicals were provided by Organon Teknika (Boxtel, The Netherlands). Solutions were prepared using phosphate-buffered saline (PBS, pH 7.4). Human chorionic gonadotrophin (hCG) and luteinizing hormone (LH) were used as antigens. Three different monoclonals of the αhCG antibody (here denoted by [1C], [7B], and [3A], respectively; isoelectric points at pH > 6) were used as well as an αLH antibody with isoelectric point at pH = 4.5. Bovine serum albumin (bSA) was used to block unoccupied sites after the initial adsorption of antibodies to avoid nonspecific adsorption of antigens. Between subsequent protein additions, the flow cell channels were flushed with PBS buffer.

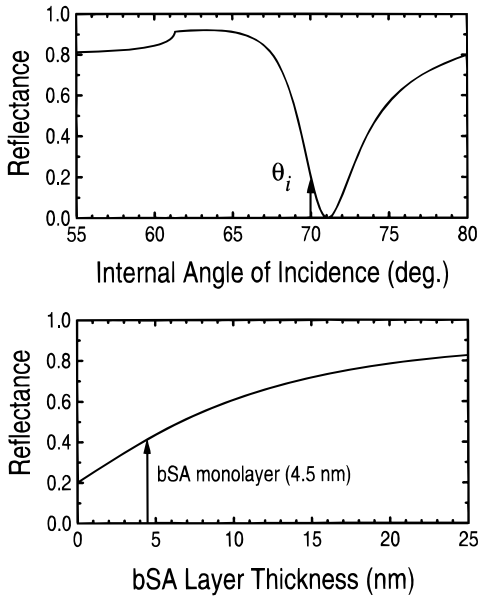


Figure 2. (a) Calculated SPR curve for a gold layer in water explaining the choice of angle of incidence $\theta_i$. As the adsorption proceeds, the SPR resonant angle will shift to the right and the reflectance at $\theta_i$ will increase (gold layer thickness, 48 nm; gold dielectric constant, 1.2*i*-12.3; wavelength, 633 nm). (b) Calculation of the reflectance as a function of the increasing protein layer thickness at $\theta_i$ (refractive index bSA, 1.45 [13]), showing the approximate linearity for layer thicknesses below 10 nm. It also shows that SPR is especially well suited for very thin layers; for thicker layers the sensitivity decreases. The absolute (normalized) reflectance change is ~0.05/nm in the range of interest (first 5 nm). The reflectance for a bSA monolayer is indicated.

## RESULTS AND DISCUSSION

**One-Dimensional Array of Sensor Surfaces.** As an initial experiment, the adsorption of BSA was measured with three different concentrations and compared to signal changes in a reference channel containing PBS only. The channels were 1 mm wide and 10 mm long, and the channel depth was about 0.1 mm. In all channels the area used for intensity determination was 4 mm long and 1 mm wide. Figure 3 shows the result of this experiment, which agrees with the expectation that adsorption speed increases with protein concentration and confirms we can measure separate adsorptions simultaneously. The lower detection limit is determined by chemical and temperature drift (compare changes in buffer signal to full bSA monolayer signal).

Having demonstrated the feasibility of a multichannel sensor based on SPR, we proceeded with real immunosensor measurements. First, the four-channels were coated with $10^{-6}$ M αhCG [7B] by adsorption to the gold surface (see Figure 4). To avoid nonspecific binding of the corresponding antigen to unoccupied areas at the gold surface, these were blocked by bSA ($10^{-5}$ M). Three different concentrations of hCG were used for the immunoreaction ($2 \times 10^{-7}$, $4 \times 10^{-8}$, and $8 \times 10^{-9}$ M). In the fourth channel, $8 \times 10^{-9}$ M LH was added, which is known to have a high cross-reactivity with αhCG because of its structural similarity with hCG.[14] Here the activity of the αhCG approximates 0.9 mol/

(13) de Feijter, J. A.; Benjamins, J.; Veer, F. A. *Biopolymers* **1978**, *17*, 1759−1772.

(14) Vaitukaitis, J. L.; Braunstein, G. D.; Ross G. T. *Am. J. Obstet. Gynecol.* **1972**, *113*, 751.

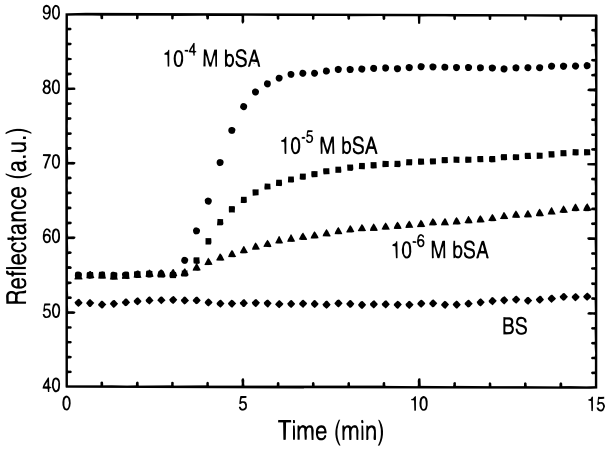


Figure 3. Four-channel adsorption experiment with bSA. The fourth channel, through which only buffer solution flowed, was used as a reference channel. The intensities as determined from the videotape are proportional to the reflectance.

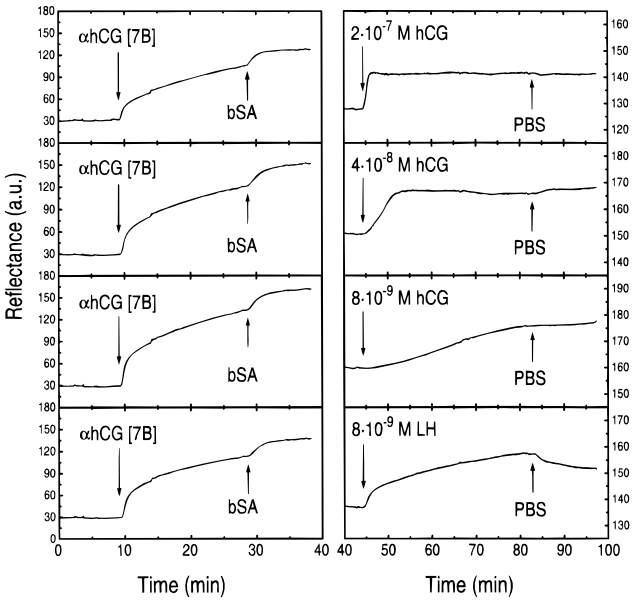


Figure 4. Four-channel immunoreaction experiment with the αhCG [7B] ($3 \times 10^{-7}$ M) in all channels. Immunoreactions were measured with three hCG concentrations and LH. Although in arbitrary units, the vertical scales of the analyte binding curves are a factor of 3 smaller than those in the antibody adsorption curves.

mol. The activity is estimated by calculating the ratio of the bound number of antibodies and antigens. The bound mass is assumed to be proportional to the change in reflectance. The molar masses were assumed to be 160 kDa for all used antibodies, 40 kDa for the antigens, and 66 kDa for bSA. In the right side of Figure 4, we see that the proceeding immunoreaction can be measured very well. The influence of the concentration on the kinetics of the immunoreaction is also apparent. The LH molecules indeed show a very high cross-reactivity with the αhCG with an activity of 0.9 mol/mol, but the measurement also shows that a significant portion of the bound LH dissociates rapidly when the flow cell is flushed with the buffer solution.

**Two-Dimensional Array of Sensor Surfaces.** An even more interesting set of measurements can be performed if a two-dimensional array of sensor surfaces is used for simultaneous measurements. Figure 5 explains the approach that was chosen:

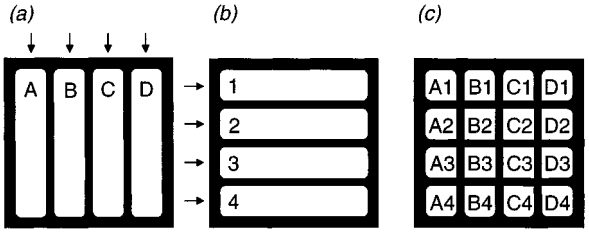


Figure 5. Schematic explanation of how to use a four-channel flow cell for 16 independent measurements in a two-dimensional array.

In a first step, the channels are coated with antibodies A−D, respectively. Then the multichannel flow cell is removed from the surface, turned 90°, and pressed to the surface again. In a second step, the antigens 1−4 are applied, flowing past the sensor areas with the different coatings. In this way, all specific reactivities and cross-reactivities can be measured in a single experiment.

Figure 6 shows the results of a two-dimensional multichannel measurement. Each of the channels was coated with $3 \times 10^{-7}$ M solution of antibody (respectively, αhCG [1C], [7B], and [3A] and αLH). All curves show a continuously increasing signal level, and adsorption kinetics and end coverage strongly depend on the type of antibody. After the remaining gold surface was blocked with bSA, the flow cell was turned 90° and analyte was applied (channels 1 and 2 contained duplicates of $2 \times 10^{-7}$ M hCG, channel 3 contained $10^{-8}$ M LH, and channel 4 acted as a reference with buffer only). Compared to Figure 4, data in column B are strongly similar, both in kinetics and in biological activity. Also note that much like in Figure 4 the cross-reacted complexes tend to fall apart easier than the specific ones when the buffer solution flows past them. Since a 4-times smaller sensing area was used (∼1 mm$^2$) the signal-to-noise ratio in the specific binding curves is smaller. Generally, the curves in Figure 6 follow the expected time behavior, although some curves exhibit drift. Again, we may estimate the biological activity of the coated antibodies, which roughly varies from 0.7 mol/mol in Figure 6 [A3] up to 1.8 mol/mol in Figure 6 [B3]. This even further shows that our measurements do provide biologically relevant information. Special attention is to be paid to the immunoactivity of the anti-LH: for both hCG and LH analytes, this IgG-type molecule shows an apparent biological activity that well exceeds the expected maximum value of 2. Given the plausible results found for all αhCG types and hCG we do not consider an instrumental artifact here but rather a biological cause. A possible explanation for this finding may be the low isoelectric point of the αLH causing ionic interaction in addition to the immunological interaction. Even though we do not understand the true biological significance of this finding, it was confirmed independently using affinity chromatography where a molar binding ratio of 4 was found from column binding capacity data. Do note that the drift effects differ for individual surface areas, thus excluding thermal causes and making chemical variations more likely.

## CONCLUSION

The feasibility of one- and two-dimensional multichannel immunosensing was demonstrated. The problem of immobilization of a number of different analytes on the multisensor surface was tackled by using a multichannel flow cell. There are other

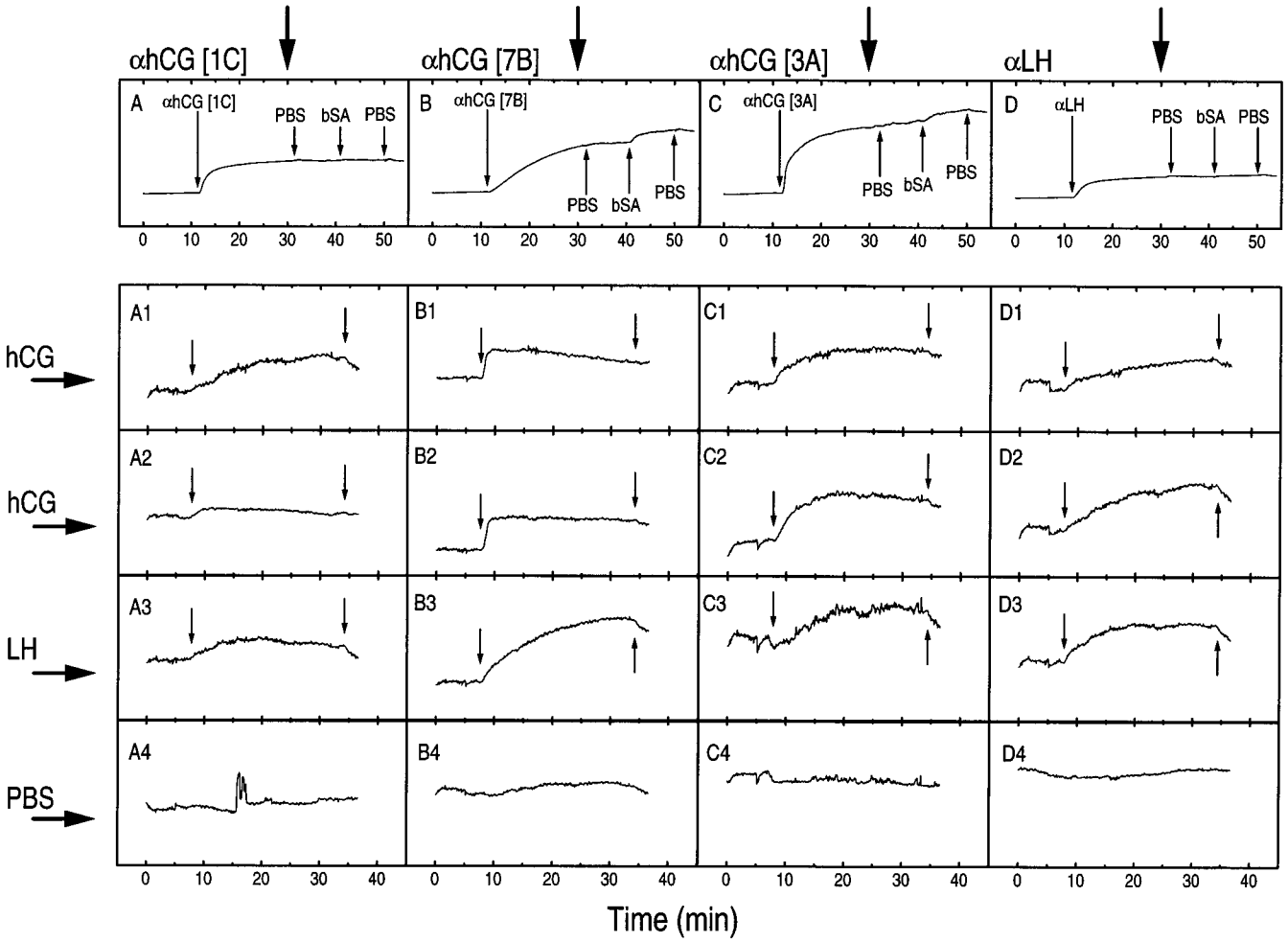


Figure 6. Two-dimensional multichannel measurement. The antibody concentrations were $3 \times 10^{-7}$ M, and the concentrations of the antigens were $2 \times 10^{-7}$ M for the hCG and $10^{-8}$ M for the LH. The first arrows in area A1 to D3 indicate when the hCG or LH was added, the second indicate the addition of PBS for washing. The vertical scales of the analyte binding curves are a factor of 3 smaller than those in the antibody adsorption curves. (Since the C3 area was defined to be smaller than the other areas, the noise level is a bit higher in the C3 data.)

ways to do this, for example, by depositing small quantities in specific locations on a sensor surface by using an ink jet nozzle.[15]

In view of the area that can be comfortably imaged (~1 $cm^2$) and the minimum area needed for read-out of one channel (~100 $\mu m^2$), an enormous number of separate, independent channels becomes available for sensor purposes. In principle, these areas can be individually covered using the above-mentioned ink jet technique; the individual addressing of channels can be done by appropriate software.

(15) Kimura, J.; Kawana, Y.; Kuriyama, T. *Biosensors* **1988**, *4*, 41−52.


## ACKNOWLEDGMENT

These investigations in the program of the Foundation for Fundamental Research on Matter (FOM) have been supported (partly) by The Netherlands Technology Foundation (STW). Andre Verhoeven (Organon Teknika) is gratefully acknowledged for his expert experimental assistance, Patrick van Breughel is thanked for his chromatography experiments on αLH.

Received for review August 26, 1997. Accepted December 4, 1997.

AC970929A